frontiers in Neurology

REVIEW
published: 21 August 2020
doi: 10.3389/fneur.2020.00801

A Radiation Oncology Approach to Brain Metastases

*N. Ari Wijetunga and T. Jonathan Yang**

Department of Radiation Oncology, Memorial Sloan-Kettering Cancer Center, New York, NY, United States

Brain metastases are a significant contributor to morbidity and mortality. The incidence of brain metastases is increasing as a result of increased time for metastasis development in the setting of improved systemic therapy and extracranial disease control and improved detection by MRI. Radiotherapy is an essential treatment modality for brain metastases in both the definitive and post-surgical adjuvant treatment contexts, and radiation oncologists rely heavily on diagnostic neuroimaging to guide treatment. Insight into the aspects of diagnostic neuroimaging that radiation oncologists rely on for clinical decision-making, radiation treatment planning, and assessment of treatment response or complications can help guide radiologists when constructing their neuroimaging reports in the context of brain metastases.

Keywords: brain metastases, radiation oncology, radiology, radiotherapy, palliation, MRI, neuroimaging

OPEN ACCESS

Edited by:
Susie Y. Huang,
Massachusetts General Hospital,
Harvard Medical School,
United States

Reviewed by:
Filippo Alongi,
University of Brescia, Italy
Jennifer Soun,
University of California, Irvine,
United States

****Correspondence:***
T. Jonathan Yang
yangt@mskcc.org

Specialty section:
This article was submitted to Applied Neuroimaging, a section of the journal Frontiers in Neurology

Received: *28 November 2019*
Accepted: *26 June 2020*
Published: *21 August 2020*

Citation:
Wijetunga NA and Yang TJ (2020) A Radiation Oncology Approach to Brain Metastases. Front. Neurol. 11:801. doi: 10.3389/fneur.2020.00801

INTRODUCTION

Brain metastases occur in as many as 25% of patients with cancer and are a significant contributor to morbidity and mortality (1). They are estimated to be symptomatic in 60–75% of patients (2) and can be associated with headaches, seizures, syncope, focal neurological deficits, gait disturbances, cognitive dysfunction, nausea, vomiting, cranial nerve dysfunction, cerebellar symptoms, and speech disturbances (3). Brain metastases arise most commonly from lung, breast, colorectal, melanoma, and renal cell primaries (4). At presentation, ∼60% of patients have multiple lesions (5). There are an estimated 200,000 incident brain metastases per year, and the incidence is increasing (6) as a result of increased time for metastasis development because of improved systemic therapy and extracranial disease control and improved detection by MRI (1, 4).

Radiation therapy (RT) plays an essential role in the management of brain metastases. The first report of the palliative benefit of whole brain radiotherapy (WBRT) was a case series by Chao et al. from Memorial Hospital (now Memorial Sloan Kettering) in 1954 that demonstrated 24 of 38 patients benefiting from WBRT (7). Several subsequent trials found that post-surgical WBRT improved overall survival, local control, and functional independence relative to WBRT alone, and RT became the standard adjuvant post-surgical treatment for brain metastases (8, 9). More recently, targeted stereotactic radiosurgery (SRS) is an increasingly useful tool for treating brain metastases while minimizing off-target brain irradiation-associated neurocognitive decline (10). When added to WBRT, SRS was demonstrated to improve overall survival in patients with a single, unresectable brain metastasis compared with WBRT alone (11). This was followed by a practice-changing trial showing that SRS with WBRT reserved for treatment failure or disease progression had equivalent overall survival compared with upfront SRS and WBRT in patients with less than five brain metastases (12). Finally, SRS without WBRT was non-inferior in treating 5–10 brain metastases when compared with 2–4 brain metastases (13). Consequently, SRS is now the favored treatment for limited brain metastases for most solid tumor histologies, defined as the number of

metastases where SRS is as effective as WBRT with more cognitive protection, whereas WBRT is used to target extensive brain disease, though it is worth noting that the National Comprehensive Cancer Network (NCCN) guidelines allow for SRS to be used for both limited and extensive brain disease (14).

In both the definitive and post-surgical adjuvant treatment contexts, radiation oncologists rely heavily on diagnostic neuroimaging to decide on a treatment course and for treatment planning. Given the panoply of features that radiologists can address when constructing their reports, there are key observations that may help to guide RT. In the following article, we will provide an overview of the radiation oncology approach to brain metastases to provide insight into specific information that may be relevant to our discipline. First, we will review the aspects of diagnostic neuroimaging that radiation oncologists rely on for clinical decision-making. Then, we will provide an overview of radiation treatment planning. Lastly, we will describe how radiation oncologists use diagnostic neuroimaging to assess treatment response, treatment-related complications, and disease recurrence.

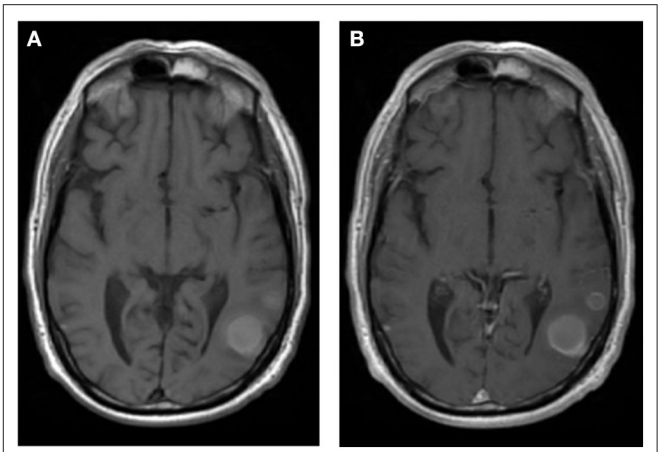

FIGURE 1 | A patient with metastatic melanoma treated with stereotactic radiosurgery (27 Gy in 3 fractions) demonstrating lesion enhancement without contrast. **(A)** T1 pre-contrast sequence demonstrating that the melanin within the tumor tends to enhance. **(B)** T1 post-contrast sequence.

Diagnostic Imaging Considerations

Brain metastases tend to occur at specific sites within the brain, and their distribution can vary by histology. For example, brain metastases are often located at the gray–white matter junction, the subarachnoid space, and the interfaces of major arterial vascular territories (15). Within the brain parenchyma, most brain metastases (up to 80%) occur in the cerebral hemispheres, whereas ∼17% occur in the cerebellum and 3% in the basal ganglia (16). Within the cerebrum, metastases tend to occur in the frontal and parietal lobes more often than in the temporal and occipital lobes (16). Uterine, prostate, and gastrointestinal cancers tend to metastasize to the posterior fossa (17).

When patients present with symptoms related to intracranial disease, CT imaging is often obtained, and it can provide initial insight into the presence of large metastases, mass effect, herniation, and hydrocephalus. Thus, CT imaging can indicate when a surgical emergency exists for which delaying care to plan RT would be inappropriate. However, CT is not the primary method for identifying and planning RT for brain metastases. Although the sensitivity of CT can be improved with contrast, CT has low sensitivity for small brain metastases relative to contrast MRI, the current gold standard for visualizing brain metastases (18, 19). Radiation oncologists typically only use CT for lesion visualization and treatment planning when MRI is contraindicated.

There are several characteristics of brain metastases that can distinguish them from primary malignancies, as well as from non-cancer abnormalities on MRI imaging. The T1 pre-contrast sequence has limited utility in visualizing most brain parenchymal metastases because brain parenchymal metastases tend to be iso-intense. However, this sequence is useful in visualizing melanoma metastases, which are T1-weighted pre-contrast hyperintense because of the presence of melanin (**Figure 1**) (20). Also, the presence of T1-weighted pre-contrast hyperintensity may indicate a hemorrhage, and lung, melanoma, choriocarcinoma, renal cell carcinoma, and thyroid carcinoma metastases are more likely to hemorrhage compared with other histologies (21). Other MR sequences such as susceptibility-weighted imaging (SWI) or gradient echo (GRE) can also detect hemorrhage and calcifications (22). The T1-weighted post-contrast sequence is essential for visualizing brain metastases. Because secondary malignancies in the brain violate the blood–brain barrier and have vasculature representative of their parent tumors (23), brain metastases generally enhance on T1-weighted post-contrast imaging, tending to appear as bright, well-demarcated, spherical masses. The center of the mass is often contrast-devoid, resulting in a rim of enhancement. Cystic metastases may appear hyperintense within the tumor on a T2-weighted sequence, whereas mucinous tumors may be T2 hypointense (24). The T2-weighted fluid-attenuated inversion recovery (FLAIR) MR sequence allows the visualization of

TABLE 1 | Summary of brain metastases imaging findings.

MRI sequence	Typical findings for brain metastases
T1 pre-contrast	Iso-intense with brain parenchyma (hemorrhage and melanoma can appear hyperintense)
T1 post-contrast	Enhancing
T1-weighted post-contrast spoiled GRE	Enhancing
T2	Variable intensity
T2 FLAIR	Hyperintense peritumoral edema
DWI	Peritumoral edema with elevated ADC compared with primary brain tumors
DTI	Anisotropy measures are lower in contrast enhancing tumor relative to primary brain tumors
SWI/GRE	Hypointense with intratumoral hemorrhage
DCE/DSC	Elevated rCBV
Spectroscopy	Choline peak within tumor and no elevation in peritumoral edema Lipid peak associated with necrosis NAA decreased

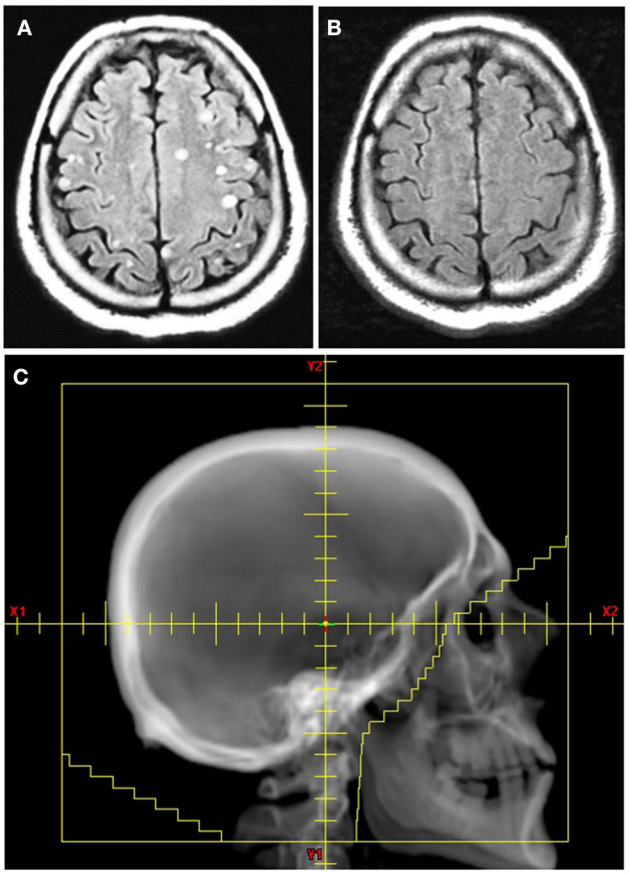

FIGURE 2 | Whole brain radiation therapy (WBRT) for a patient with non-small cell lung cancer with multiple brain metastases. **(A)** T2 FLAIR axial image before WBRT. **(B)** T2 FLAIR axial image 6 months after WBRT with 30 Gy in 10 fractions. **(C)** Radiation field for WBRT defined using the skull anatomy.

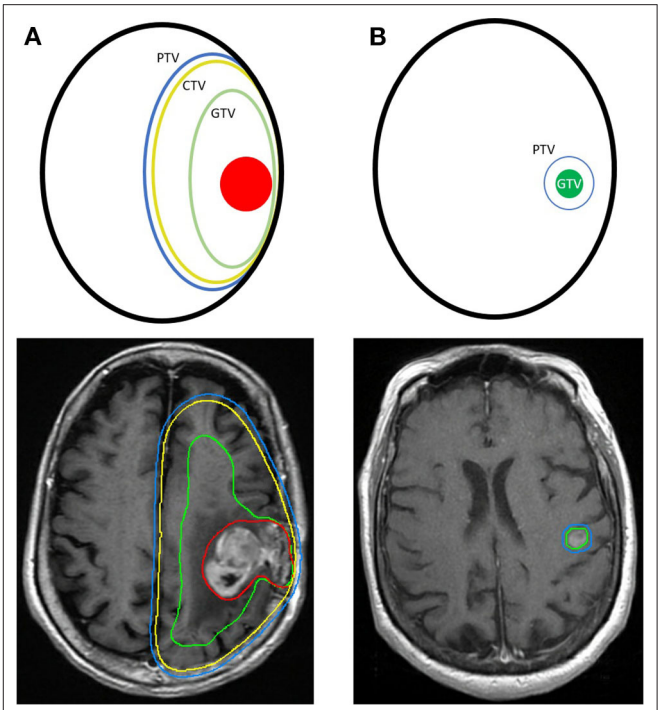

FIGURE 3 | Comparison of the radiation planning treatment volumes for a primary malignancy and stereotactic radiosurgery (SRS) for a brain metastasis. **(A)** A primary glioblastoma multiforme with a GTV, *green*, encompassing the gross tumor, *red*, and edema. A CTV, *yellow*, and PTV, *blue*, are shown as concentric expansions from the GTV. **(B)** A metastatic brain lesion treated with SRS and a GTV, *green*, with a PTV, *blue*. No CTV is required because of low risk of tumor invasion into the brain parenchyma.

peritumoral edema. Diffusion-weighted imaging (DWI) is an area of interest because metastases and gliomas have different apparent diffusion coefficients (ADCs) compared with normal brain matter, although there is considerable overlap between the ADCs of primary brain tumors, metastases, edema, and non-tumoral lesions (25). DWI can potentially distinguish gliomas from brain metastases because the mean minimum ADC within the vasogenic edema of metastases was found to be higher than that of the infiltrative edema of gliomas (26). Conversely, in dynamic contrast-enhanced (DCE) perfusion MR imaging, the relative cerebral blood volume (rCBV) of peritumoral edema for gliomas tends to be significantly greater than that of brain metastases (27). The typical MRI findings for brain metastases are summarized in **Table 1**.

Primary brain malignancies and non-cancer abnormalities have specific characteristics on diagnostic imaging that allow for their identification relative to brain metastases. Both gliomas and brain metastases tend to have low signal on T1-weighted sequences and high signal on T2-weighted sequences, making it difficult to distinguish between gliomas and brain metastases on this basis. However, gliomas tend to form expansile masses that conform to the barriers of the lobe or deep nuclear structures, whereas brain metastases are well demarcated. Because most brain metastases are contrast enhancing, enhancement can also aid in distinguishing gliomas from brain metastases depending on glioma grade. Approximately 70% of high-grade gliomas are contrast enhancing, whereas only 20% of low-grade gliomas are (28). Like gliomas, non-cancer brain abnormalities visible on imaging, including infarcts, demyelinating plaques, abscesses, hematomas, necrosis, and encephalitis, may also be confused with metastases (29). These entities can demonstrate contrast enhancement, perilesional edema, mass effect, and central necrosis. Acute infarcts can appear as masses with contrast enhancement on CT, like brain metastases; however, infarcts show evolving changes over time on repeat MRIs. T1-weighted and T2-weighted MRI sequences are less useful in the acute setting because they show abnormalities in <50% of acute infarct cases, whereas techniques like perfusion imaging and DWI can show differences within minutes of symptom onset (30). In the subacute and chronic settings, infarcted brain is associated with high extracellular fluid content and increased T2-weighted MRI signal. Abscesses are difficult to distinguish from brain metastases, appearing as round lesions with associated edema and ring-like peripheral contrast enhancement (31). DWI can

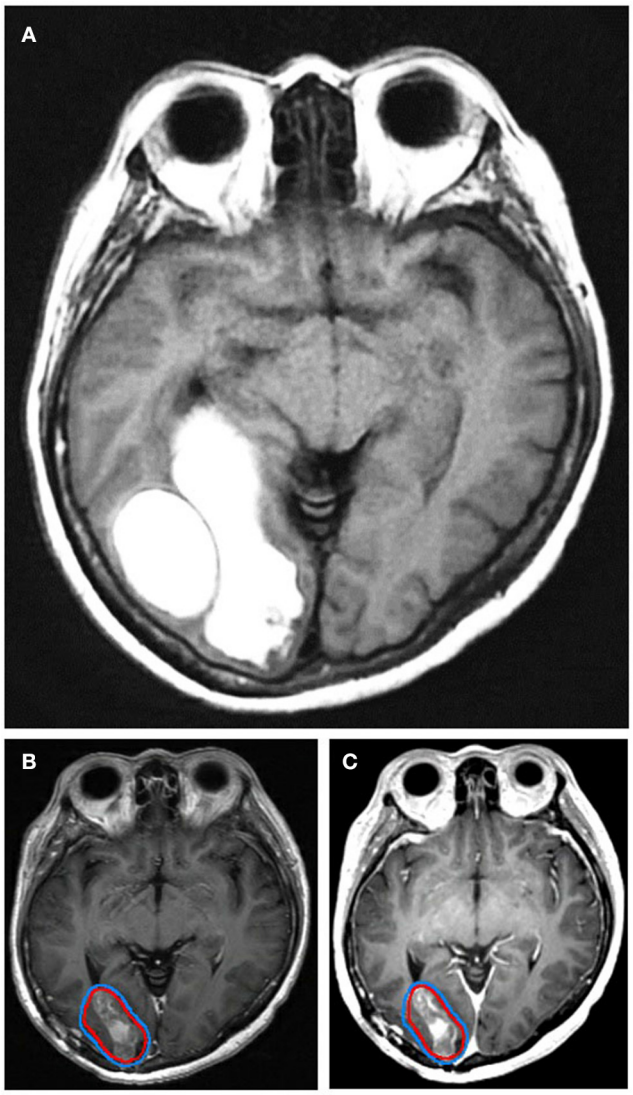

FIGURE 4 | A patient with a non-small cell lung cancer metastasis shown **(A)** preoperatively, **(B)** postoperatively on T1-post weighted MRI, and **(C)** on 3D brain volume (BRAVO) MRI. The postoperative cavity is contoured as the GTV, *red*, with an expansion to the PTV, *blue*. The patient was treated with stereotactic radiosurgery and 27 Gy in 3 fractions.

help to distinguish abscesses and tumors because abscesses have restricted diffusion in their center from the high cellularity and viscosity of pus relative to brain metastases, although mucinous and highly cellular brain metastases may also have central restricted diffusion (32). Necrosis can be the result of a malignancy or a side effect from radiation (see Post-radiation evaluation). It is considered a hallmark of high-grade gliomas, like glioblastoma multiforme, whereas it is relatively uncommon in the setting of a small, treatment-naive brain metastasis. Both necrosis and tumor can appear T2 hyperintense and contrast enhancing, so conventional MRI may fail to distinguish them (33). However, recent advances in MRI have shown a potential for differentiating necrosis from tumors, such as MR spectroscopy and amide proton transfer (APT) MR. APT MR can detect the amide protons of low-concentration mobile proteins and peptides in the cytoplasm of necrotic cells, thus differentiating necrosis from brain tumors (34).

TABLE 2 | Typical point dose constraints for organs at risk.

Organ	Total dose (Gy)
Brainstem	55
Cochlea	50
Cord	50
Lacrimal gland	40
Lens	10
Optic chiasm	54
Optic nerve	54
Pituitary	60
Retina	45

Radiation Planning and Treatment Considerations

According to the NCCN guidelines, the type and timing of RT for brain metastases depends on the clinical scenario, including the number and volume of metastases, the dose and fractionation of planned radiation, systemic treatment options, and the anticipated benefit of surgical resection (35). If a brain metastasis is >2 cm, or if the patient is acutely symptomatic from the brain metastasis, they may be referred for surgery before RT (36). The benefit of surgical resection depends on the need for tissue diagnosis, the size and location of the lesion, and the institutional experience. As SRS is a treatment option for limited brain metastases (13), at our institution, SRS is the preferred treatment method for limited brain metastases when patients have new or stable systemic disease and have additional systemic treatment options. In the setting of multiple brain metastases, the NCCN recommends SRS over WBRT if the patient has a good performance status, radioresitant histology, or low overall tumor volume. When 116 radiation oncologists were surveyed for the "maximum number of brain metastases [they] would commonly treat with upfront SRS without offering WBRT," 40.4% indicated 1–4, 42.1% indicated 5–10, 14% indicated 10–20, and 3.5% did not have a limit (37). Furthermore, when asked what other factors influenced this decision, the location and histology of the metastases mattered the most. In a similar survey, the average cutoff for switching from SRS to WBRT was 8.1 brain metastases for central nervous system (CNS) specialists with a high clinical volume compared with 4.9 brain metastases for CNS specialists with a low clinical volume (38). An example of a WBRT plan for a patient with numerous brain metastases as well as the response to the treatment is shown in **Figure 2**.

The first step in planning RT is a CT (also known as a radiation simulation) with the patient in the treatment position and appropriate immobilization devices, such as a rigid, custom-made thermoplastic mask and headrest. Using the planning

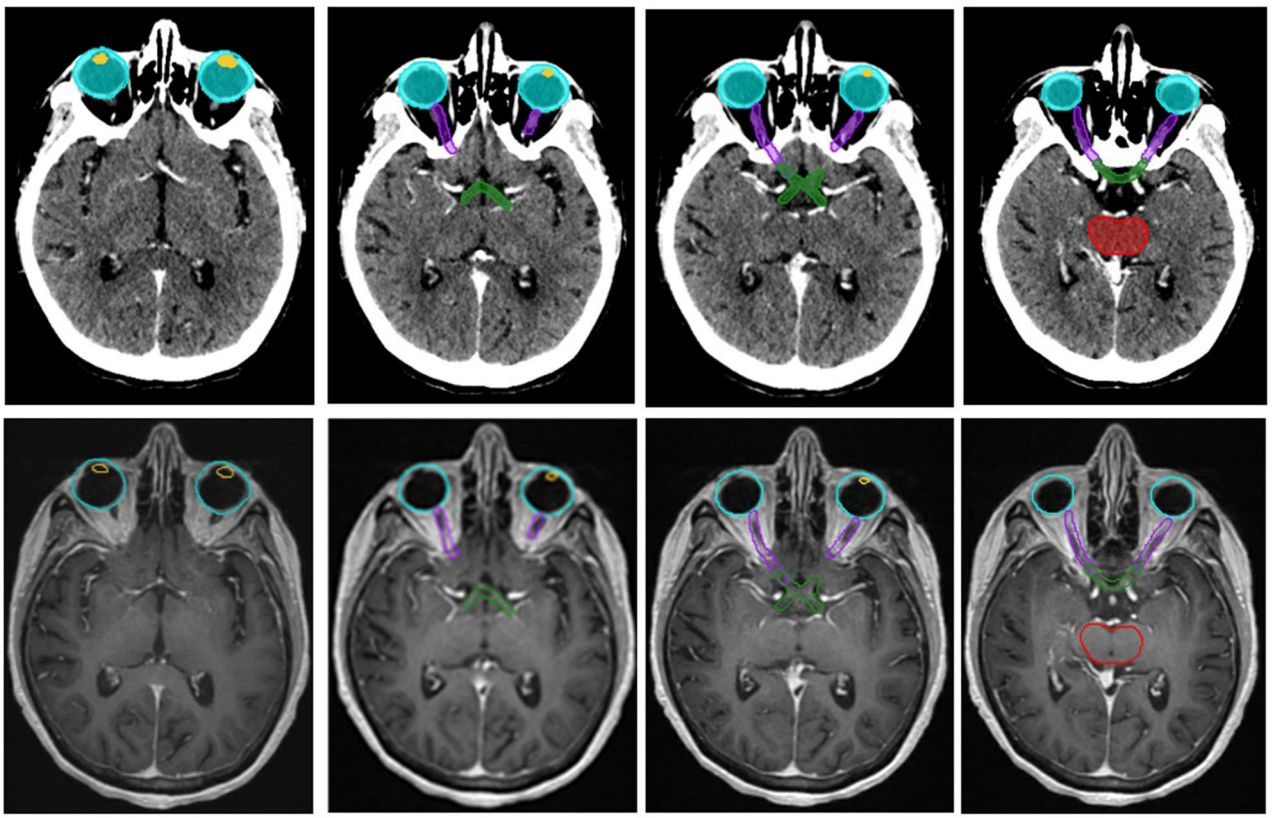

FIGURE 5 | Organs at risk (OARs) defined on a planning CT and corresponding T2-weighted MR images. The included OARs are the lenses, *yellow*, the eyes, *aqua*, the optic nerves, *purple*, the optic chiasm, *green*, and the brain stem, *red*.

CT in conjunction with MRI, radiation oncologists define the radiation treatment area primarily using three target volumes. The gross tumor volume (GTV) encompasses all visible disease. The clinical target volume (CTV) includes the GTV, but it also accounts for subclinical disease spread. The CTV is often an expansion beyond the GTV that respects anatomical borders and can include areas at risk for microscopic disease (e.g., including involved cranial nerves in the case of observed neurotropism). However, for metastatic lesions to the brain, the expansion from GTV to CTV is usually 0 mm as there is no expected subclinical extension of disease. Finally, the planning target volume (PTV) is an expansion on the CTV that accounts for daily setup uncertainties (39). Modern RT techniques include positioning devices specifically designed for neuroradiation and onboard imaging (daily 2D and 3D imaging) that allows for high accuracy of treatment and results in minimal patient setup uncertainties, thus allowing the PTV margin to be as small as 0–2 mm. An example of GTV, CTV, and PTV volumes for a typical brain metastasis SRS case compared with a primary malignancy case can be seen in **Figure 3**. In the postoperative setting, the T1 post-contrast image from the postoperative MRI is used to define a GTV as enhancing disease. If there is no enhancing disease, the postoperative cavity is contoured as a CTV. An expansion is made to the PTV directly from a GTV, in the case of residual tumor, or from CTV, in the case of gross resection, using a margin of 2–3 mm. An example of a postoperative SRS case can be seen in **Figure 4**.

In planning RT for brain metastases, radiation oncologists typically request an MRI with contrast and 1-mm slice thickness for optimal visualization of the metastases. Ideally, the patient will be immobilized during the MR with the same mask that is used for the planning CT, which will allow for near-perfect registration of the two imaging studies for contouring and treatment planning. For WBRT, no fusion is typically needed, as the anatomical borders of the brain will determine the borders of the treatment fields. However, MRI fusion is required for hippocampal-sparing WBRT, a technique associated with memory preservation and improved quality of life, to ensure the lack of visible metastases in the bilateral hippocampal regions and for accurate contouring (40). For SRS planning, the T1-weighted post-contrast sequence is generally able to visualize the metastases. A T1-weighted post-contrast spoiled GRE sequence, known for high spatial resolution to display anatomical structures of both normal brain and tumors (41) and to detect small brain metastases (42), is also often requested. These two MR sequences are fused to the planning CT, and a GTV is contoured encompassing the visible lesion with a 0–2 mm expansion to PTV.

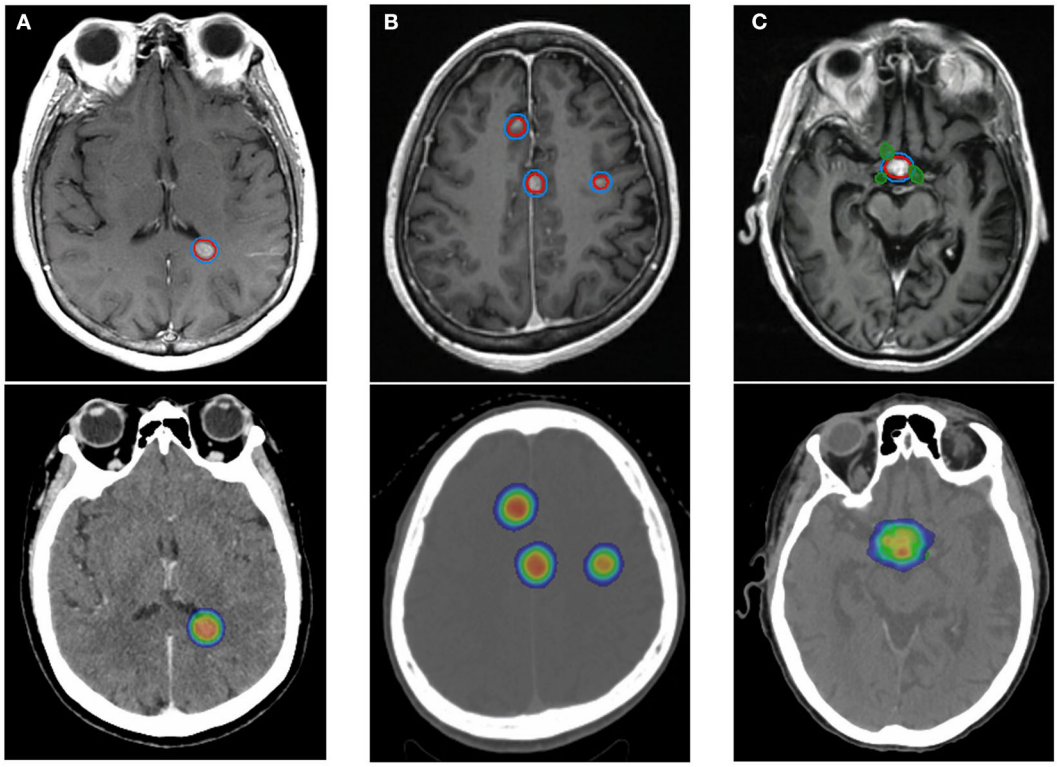

FIGURE 6 | The planning target volumes and corresponding radiation plan for three patients using stereotactic radiosurgery and altered fractionation depending on number and location of metastases relative to organs at risk. **(A)** A patient with a single brain metastasis treated with 21 Gy in 1 fraction. No organs at risk fall within the treatment fields. **(B)** A patient with multiple brain metastases, each treated with 27 Gy in 3 fractions. The lesions are close to one another and are located at the midline. **(C)** A patient with a single brain metastasis overlying the optic chiasm, *green*, treated with 30 Gy in 5 fractions. GTV, *red*. PTV, *blue*. The radiation dose gradient depicts 10 Gy as *blue* and >100% of prescribed dose as *orange*.

To safely deliver radiation to the brain, it is important to note the proximity of a tumor to organs at risk (OARs). The doses to OARs are constrained according to empirically derived limits and can vary by institution and study group. Whether the mean radiation dose to the organ or the maximum point dose to the organ is constrained during radiation planning depends on whether the organ functions serially (such as the brainstem), in parallel (such as the brain parenchyma), or both. The common OARs that are constrained in the head are the lens, eyes, lacrimal glands, optic nerves, optic chiasm, cochlea, pituitary, and brainstem (**Table 2**). Each structure is carefully contoured during treatment planning so that toxicities are limited (**Figure 5**). The proximity of a tumor to an OAR will alter a planned dose and fractionation so that dose limits are not exceeded, and patients are spared risk of toxicity (**Figure 6**). MR imaging can detect toxicity to OARs after RT. For example, decreased white matter fiber integrity in the para-hippocampal cingulum after brain irradiation demonstrated by MR diffusion tensor imaging (DTI) is thought to relate to late cognitive decline (43).

Post-radiation Evaluation

Patients are usually evaluated every 2–3 months for 1–2 years after RT with high-resolution MRI to determine treatment response and are followed by interval scans every 4–6 months thereafter. The Response Assessment in Neuro-Oncology group defined treatment response using criteria that include T1 gadolinium enhancing disease, T2 and FLAIR changes, the appearance of new lesions, corticosteroid requirement, and clinical status. Evaluation of treatment response can be complicated by several factors, including radiation inflammation, radionecrosis, and recurrence of the tumor (44). Post-radiation changes to tumors and normal tissue vary over time and are typically observed as acute (during or immediately following RT), subacute (within 3 months of RT), or late (months to years after RT). Acute-onset encephalopathy related to RT may not have associated imaging findings but will likely have associated symptoms that will prompt neuroimaging, such as headache, nausea, vomiting, fever, altered mental status, worsening neurologic symptoms, and increased intracranial pressure. It is estimated that ∼5% of patients receiving SRS to the brain will present with acute neurotoxicity (45), and MRI can show varying amounts of edema. Depending on the imaging findings and the severity of symptoms, high-dose steroids can often improve the acute effects of brain irradiation, and, occasionally, surgery is warranted. Subacute radiation effects include increased inflammation, which may cause a tumor

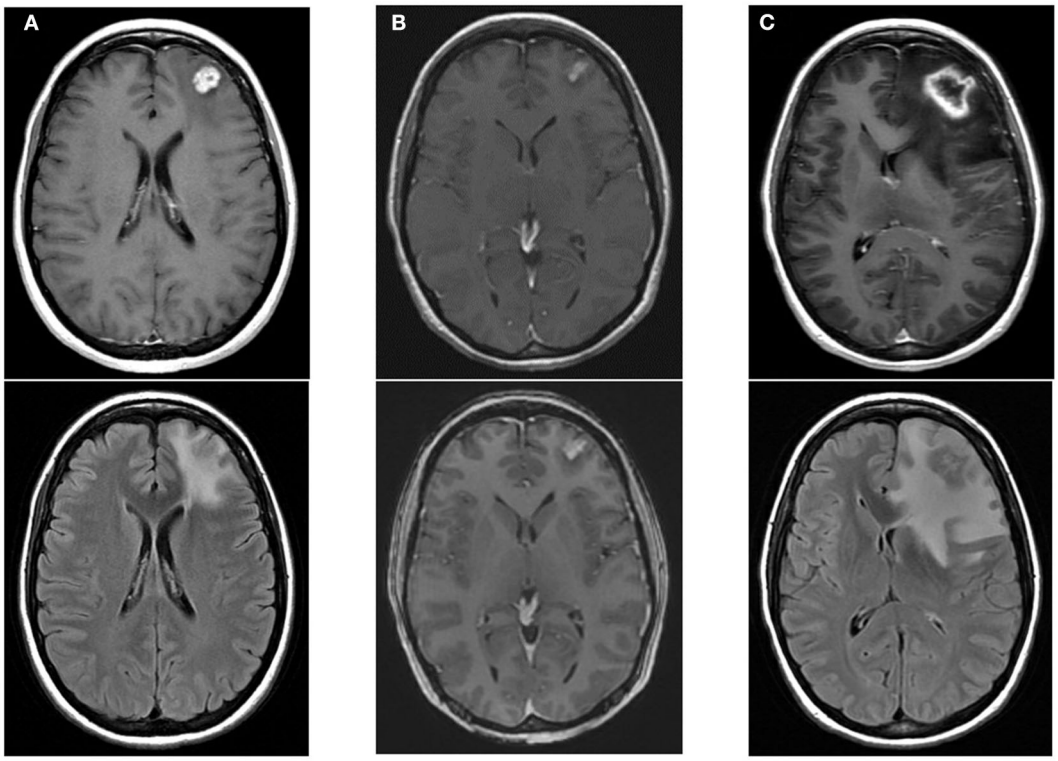

FIGURE 7 | An example of radiation necrosis after stereotactic radiosurgery with 21 Gy in 1 fraction with upper images showing T1-post contrast and the lower images showing edema. **(A)** Pre-radiotherapy scans showing a left frontal metastasis. **(B)** 2 months post-RT scans showing contraction of the treated metastasis with some effacement of the ventricles. **(C)** 6 months post-RT peripheral enhancement of treated metastasis with a necrotic center and associated edema, ultimately requiring surgical intervention.

to appear larger on MRI than it was before radiation. In addition, some chemotherapies, such as temozolomide, can cause pseudoprogression in the subacute context, making irradiated brain lesions look like they have progressed on MRI when they have not (46). If a patient with suspected pseudoprogression is asymptomatic, they are typically monitored with follow-up MRI to rule out genuine disease progression. Late changes after radiation include stabilization or contraction of the observed lesion if there has been treatment response. MR SWI sequences can show microbleeds after radiation that increase in frequency over time (47). In the subacute to late setting, potentially symptomatic radiation necrosis can also occur, with mass effect and neurologic dysfunction.

Radiation oncologists often rely on MRI to identify radiation necrosis. Radiation necrosis is hypothesized to be related to vascular injury and glial and white matter damage, as well as effects on the fibrinolytic enzyme system and immune mechanisms (48). The volume of irradiated brain increases the risk of this serious complication (49, 50). In a study of 206 patients with 310 brain metastases treated with SRS, radiation necrosis was observed in 24% of treated lesions, and roughly half were asymptomatic, unlikely to have been detected in the absence of MRI (49). Moreover, in autopsy studies of patients who underwent SRS for brain metastases, necrosis was noted as early as 3 weeks after treatment (51). Some indications of radiation necrosis that are noted on MRI are conversion from non-enhancing to enhancing lesions, new periventricular enhancement, and soap-bubble or Swiss cheese enhancement (48). To correctly distinguish necrosis from tumor recurrence, it is likely that multiple MRI sequences will be needed (52). There is some evidence that the DTI anisotropy ratio of a contrast-enhanced lesion is significantly lower in patients with radiation necrosis than in those with recurrent tumor, and facilitated diffusion favors radiation necrosis (53). MR spectroscopy, which can interrogate the chemical content of a volume of tissue may be useful in differentiating radiation necrosis from disease recurrence. Because necrotic tissue and treated tumor should have different metabolic profiles, identifying metabolic spectra can differentiate necrosis and treatment response (54). There is also some evidence of elevated lipid levels in necrotic brain tissue that may be detectable on MR spectroscopy (55). As tumors are generally more metabolically active than necrotic tissue, fluorine-18 fluorodeoxyglucose (FDG) PET-CT activity can also help distinguish progression relative to radiation injury, though it is not as predictive as perfusion imaging (56). An example of radiation necrosis after SRS is shown in **Figure 7**.

A recurrent brain metastasis can be obscured by post-treatment inflammation and radionecrosis, so it is important to

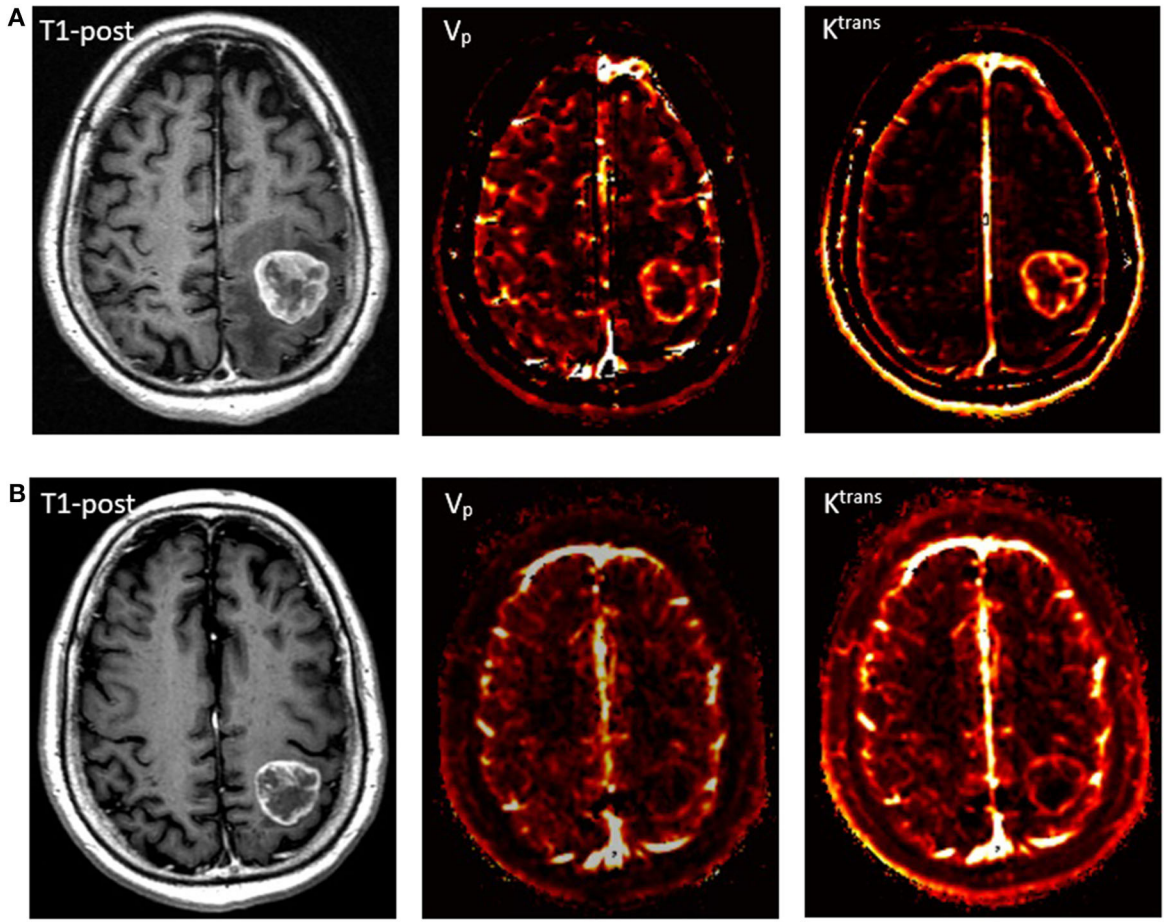

FIGURE 8 | Perfusion imaging of a patient with metastatic squamous cell carcinoma. **(A)** A pre-treatment T1-post contrast MRI with corresponding V_p and K^{trans} perfusion imaging demonstrating increased signal. **(B)** 2-month follow-up scan after receiving SRS with 27 Gy in 3 fractions showing slight contraction of the mass on T1-post MRI and marked decrease in perfusion.

carefully rule out these side effects during follow-up imaging. Because DCE MRI can provide insight into tumor vascularity and hemodynamics, plasma volume (V_p) and the volume transfer coefficient (K^{trans}) can aid in deciphering brain metastasis recurrence during post-treatment diagnostic imaging. These MR sequences use a two-compartment kinetic model, where contrast is initially assumed to be within the blood plasma volume and, over time, it leaks into the interstitial space. V_p approximates tumor vascularity, and K^{trans} is proportional to the accumulation of contrast in the interstitial space, where it can indicate increased permeability. In contrast to gliomas that can produce molecules such as VEGF that disrupt the blood–brain barrier (57), metastatic disease generally does not affect the surrounding vascularity of the brain. Therefore, an increase in V_p after radiation, when the V_p signal was previously noted to nadir, is correlated with tumor recurrence (56). Elevated K^{trans} signal has also been associated with tumor recurrence compared with treatment-induced necrosis (58), and the combination of V_p and K^{trans} signals together can further improve sensitivity and specificity (56). An example of post-RT perfusion imaging is shown in **Figure 8**. Dynamic susceptibility contrast (DSC) MRI has similar perfusion parameters to DCE MRI, such as rCBV, but it is not preferred over DCE MRI because of worse spatial resolution and more artifacts (59). Like V_p and K^{trans}, elevated rCBV is shown to indicate recurrent metastatic tumors after brain SRS (60). As is the case with radionecrosis, in MR spectroscopy, the metabolic spectra of enhancing edema may be able to differentiate tumor recurrence. For example, *N*-acetyl aspartate (NAA) is suppressed and choline is elevated in both high-grade primary malignancies and secondary brain tumors; however, only the edema associated with primary tumors tends to have a relative increase in choline (61).

CONCLUSION

In the USA, radiation oncology split from diagnostic radiology training in 1969, as it was recognized that radiation oncology training should be specialized to accommodate increasing cancer detection, new imaging modalities, and improved radiation delivery. Because radiation oncologists often do not receive formal diagnostic radiology training, they are instead expected to partner with diagnostic radiologists, who can provide important

insight to guide clinical decision-making. As Sarah Donaldson, a former president of the Radiologic Society of North America and radiation oncologist, wrote, "[Radiation oncologists] need to see and measure tumors in every dimension, understand how tumors move, their heterogeneity, their blood supply, and their molecular pathways. More than ever before in the history of radiology, radiation oncologists have an intensely strong interrelationship that already aligns radiologists as partners." (62) Though there have been numerous advances in imaging, including MRI with DWI, DTI, SWI/GRE, DCE/DSC, MR spectroscopy, and APT MR, these methods are not always incorporated into clinical decision-making by radiation oncologists. Thus, the close partnership between radiologists and radiation oncologists will allow these exciting technologies to become commonplace in radiation oncology clinical practice and, ultimately, lead to earlier brain metastases detection, improved radiotherapy treatment planning, more accurate treatment delivery, and optimal post-therapy monitoring.

AUTHOR CONTRIBUTIONS

NW and TY both evaluated the scientific literature and wrote the review together. Both authors contributed to the article and approved the submitted version.

FUNDING

Funding support for this study was provided by the National Institute of Health (NIH), NIH-NCI U54CA137788/U54CA132378.

REFERENCES

1. Gavrilovic I, Posner J. Brain metastases: epidemiology and pathophysiology. *J Neurooncol*. (2005) 75:5–14. doi: 10.1007/s11060-004-8093-6
2. Soffietti R, Cornu P, Delattre JY, Grant R, Graus F, Grisold W, et al. EFNS Guidelines on diagnosis and treatment of brain metastases: report of an EFNS Task Force. *Eur J Neurol*. (2006) 13:674–81. doi: 10.1111/j.1468-1331.2006.01506.x
3. Chang E, Lo S. Diagnosis and management of central nervous system metastases from breast cancer. *Oncologist*. (2003) 8:398–410. doi: 10.1634/theoncologist.8-5-398
4. Barnholtz-Sloan JS, Sloan AE, Davis FG, Vigneau FD, Lai P, Sawaya RE. Incidence proportions of brain metastases in patients diagnosed (1973 to 2001) in the Metropolitan Detroit Cancer Surveillance System. *J Clin Oncol*. (2004) 22:2865–72. doi: 10.1200/JCO.2004.12.149
5. DeAngelis L. Management of brain metastases. *Cancer Investig*. (1994) 12:156–65. doi: 10.3109/07357909409024871
6. Schouten LJ, Rutten J, Huveneers HA, Twijnstra A. Incidence of brain metastases in a cohort of patients with carcinoma of the breast, colon, kidney, and lung and melanoma. *Cancer*. (2002) 94:2698–705. doi: 10.1002/cncr.10541
7. Chao J, Phillips R, Nickson JJ. Roentgen-ray therapy of cerebral metastases. *Cancer*. (1954) 7:682–9. doi: 10.1002/1097-0142(195407)7:4<682::AID-CNCR2820070409>3.0.CO;2-S
8. Patchell R, Tibbs PA, Regine WF, Dempsey RJ, Mohiuddin M, Kryscio RJ, et al. Postoperative radiotherapy in the treatment of single metastases to the brain: a randomized trial. *JAMA*. (1998) 280:1485–9. doi: 10.1001/jama.280.17.1485
9. Noordijk EM, Vecht CJ, Haaxma-Reiche H, Padberg GW, Voormolen JH, Hoekstra FH, et al. The choice of treat-ment of single brain metastasis should be based on extracranial tumoractivity and age. *Int J Radiat Oncol Biol Phys*. (1994) 29:711–7. doi: 10.1016/0360-3016(94)90558-4
10. Shinde A, Akhavan D, Sedrak M, Glaser S, Amini A. Shifting paradigms: whole brain radiation therapy versus stereotactic radiosurgery for brain metastases. *CNS Oncol*. (2019) 8:1. doi: 10.2217/cns-2018-0016
11. Andrews DW, Scott CB, Sperduto PW, Flanders AE, Gaspar LE, Schell MC, et al. Whole brain radiation therapy with or without stereotactic radiosurgery boost for patients with one to three brain metastases: phase III results of the RTOG 9508 randomised trial. *Lancet*. (2004) 363:1665–72. doi: 10.1016/S0140-6736(04)16250-8
12. Aoyama H, Shirato H, Tago M, Nakagawa K, Toyoda T, Hatano K, et al. Stereotactic radiosurgery plus whole-brain radiation therapy vs stereotactic radiosurgery alone for treatment of brain metastases: a randomized controlled trial. *JAMA*. (2006) 295:2483–91. doi: 10.1001/jama.295.21.2483
13. Yamamoto M, Serizawa T, Shuto T, Akabane A, Higuchi Y, Kawagishi J, et al. Stereotactic radiosurgery for patients with multiple brain metastases (JLGK0901): a multi-institutional prospective observational study. *Lancet Oncol*. (2014) 15:387–95. doi: 10.1016/S1470-2045(14)70061-0
14. National Comprehensive Cancer Network Clinic Practice Guidelines in Oncology. *Central Nervous System Cancers* (Version 3.2019) (2019). Available online at: https://www.nccn.org/professionals/physician_gls/pdf/cns.pdf (accessed November 23, 2019).
15. Cha S. Update on brain tumor imaging: from anatomy to physiology. *Am J Neuroradiol*. (2006) 27:475–87. Available online at: http://www.ajnr.org/content/27/3/475.long
16. Hwang T, Close T, Grego J, Brannon W, Gonzales F. Predilection of brain metastasis in gray and white matter junction and vascular border zones. *Cancer*. (1996) 77:1551–5. doi: 10.1002/(SICI)1097-0142(19960415)77:8<1551::AID-CNCR19>3.0.CO;2-Z
17. Delattre JY, Krol G, Thaler HT, Posner JB. Distribution of brain metastases. *Arch Neurol*. (1988) 45:741–4. doi: 10.1001/archneur.1988.00520310047016
18. Graif M, Bydder GM, Steiner RE, Niendorf P, Thomas DG, Young IR. Contrast-enhanced MR imaging of malignant brain tumors. *AJNR*. (1985) 6:855–62.
19. Sze G, Milano E, Johnson C, Heier L. Detection of brain metastases: comparison of contrast-enhanced MR with unenhanced MR and enhanced CT. *Am J Neuroradiol*. (1990) 11:785–91.
20. Isiklar I, Leeds NE, Fuller GN, Kumar AJ. Intracranial metastatic melanoma: correlation between MR imaging characteristics and melanin content. *Am J Roentgenol*. (1995) 165:1503–12. doi: 10.2214/ajr.165.6.7484597
21. Fink KR, Fink JR. Imaging of brain metastases. *Surg Neurol Int*. (2013) 4:S209–19. doi: 10.4103/2152-7806.111298
22. Wycliffe ND, Choe J, Holshouser B, Oyoyo UE, Haacke EM, Kido DK. Reliability in detection of hemorrhage in acute stroke by a new three-dimensional gradient recalled echo susceptibility-weighted imaging technique compared to computed tomography: a retrospective study. *J Magn Reson Imaging*. (2004) 20:372–7. doi: 10.1002/jmri.20130
23. Long DM. Capillary ultrastructure in human metastatic brain tumors. *J Neurosurg*. (1979) 51:53–8. doi: 10.3171/jns.1979.51.1.0053
24. Oshiro S, Tsugu H, Komatsu F, Abe H, Ohmura T, Sakamoto S, et al. Metastatic adenocarcinoma in the brain: magnetic resonance imaging with pathological correlations to mucin content. *Anticancer Res*. (2008) 28:407–13. Available online at: http://ar.iiarjournals.org/content/28/1B/407.long
25. Maier SE, Sun Y, Mulkern RV. Diffusion imaging of brain tumors. *NMR Biomed*. (2010) 23:849–64. doi: 10.1002/nbm.1544
26. Lee EJ, terBrugge K, Mikulis D, Choi DS, Bae JM, Lee SK, et al. Diagnostic value of peritumoral minimum apparent diffusion coefficient for differentiation of glioblastoma multiforme from solitary metastatic lesions. *Am J Roentgenol*. (2011) 196:71–6. doi: 10.2214/AJR.10.4752
27. Law M, Cha S, Knopp EA, Johnson G, Arnett J, Litt AW. High-grade gliomas and solitary metastases: differentiation by using

perfusion and proton spectroscopic MR imaging. *Radiology*. (2002) 222:715–21. doi: 10.1148/radiol.2223010558
28. Silverman C, Marks JE. Prognostic significance of contrast enhancement in low-grade astrocytomas of the adult cerebrum. *Radiology*. (1982) 139:211–3. doi: 10.1148/radiology.139.1.7208924
29. Stadnik TW, Demaerel P, Luypaert RR, Chaskis C, Van Rompaey KL, Michotte A, et al. Imaging tutorial: differential diagnosis of bright lesions on diffusion-weighted MR images. *Radiographics*. (2003) 23:e7. doi: 10.1148/rg.e7
30. Kidwell CS, Villablanca JP, Saver JL. Advances in neuroimaging of acute stroke. *Curr Atheroscler Rep*. (2000) 2:126–35. doi: 10.1007/s11883-000-0107-z
31. Huisman TA. Tumor-like lesions of the brain. *Cancer Imaging*. (2009) 9A:S10. doi: 10.1102/1470-7330.2009.9003
32. Schaefer PW. Applications of DWI in clinical neurology. *J Neurol Sci*. (2001) 186:S25–35. doi: 10.1016/S0022-510X(01)00488-9
33. Dooms GC, Hecht S, Brant-Zawadzki M, Berthiaume Y, Norman D, Newton TH. Brain radiation lesions: MR imaging. *Radiology*. (1986) 158:149–55. doi: 10.1148/radiology.158.1.3940373
34. Zhou J, Tryggestad E, Wen Z, Lal B, Zhou T, Grossman R, et al. Differentiation between glioma and radiation necrosis using molecular magnetic resonance imaging of endogenous proteins and peptides. *Nat Med*. (2011) 17:130. doi: 10.1038/nm.2268
35. National Comprehensive Cancer Network Clinic Practice Guidelines in Oncology. *Central Nervous System Cancers* (Version 3.2019) (2019). Available online at: https://www.nccn.org/professionals/physician_gls/pdf/cns.pdf (accessed November 23, 2019).
36. Ewend MG, Morris DE, Carey LA, Ladha AM, Brem S. Guidelines for the initial management of metastatic brain tumors: role of surgery, radiosurgery, and radiation therapy. *J Natl Compr Cancer Netw*. (2008) 6:505–14. doi: 10.6004/jnccn.2008.0038
37. Blomain ES, Kim H, Garg S, Bhamidipati D, Guo J, Kalchman I, et al. Stereotactic radiosurgery practice patterns for brain metastases in the United States: a national survey. *J Radiat Oncol*. (2018) 7:241–6. doi: 10.1007/s13566-018-0353-8
38. Sandler KA, Shaverdian N, Cook RR, Kishan AU, King CR, Yang I, et al. Treatment trends for patients with brain metastases: does practice reflect the data? *Cancer*. (2017) 123:2274–82. doi: 10.1002/cncr.30607
39. Purdy JA. Current ICRU definitions of volumes: limitations and future directions. *Semin Radiat Oncol*. (2004) 14:27–40. doi: 10.1053/j.semradonc.2003.12.002
40. Gondi V, Tomé WA, Mehta MP. Why avoid the hippocampus? A comprehensive review. *Radiother Oncol*. (2010) 97:370–6. doi: 10.1016/j.radonc.2010.09.013
41. Hou BL, Hu J. MRI and MRS of human brain tumors. *Tumor Biomark Discov*. (2009) 520:297–314. doi: 10.1007/978-1-60327-811-9_21
42. Nagai A, Shibamoto Y, Mori Y, Hashizume C, Hagiwara M, Kobayashi T. Increases in the number of brain metastases detected at frame-fixed, thin-slice MRI for gamma knife surgery planning. *Neuro Oncol.* (2010) 12:1187–92. doi: 10.1093/neuonc/noq084
43. Chapman CH, Nagesh V, Sundgren PC, Buchtel H, Chenevert TL, Junck L, et al. Diffusion tensor imaging of normal-appearing white matter as biomarker for radiation-induced late delayed cognitive decline. *Int J Radiat Oncol Biol Phys*. (2012) 82:2033–40. doi: 10.1016/j.ijrobp.2011.01.068
44. Lin NU, Lee EQ, Aoyama H, Barani IJ, Barboriak DP, Baumert BG, et al. Response assessment criteria for brain metastases: proposal from the RANO group. *lancet Oncol.* (2015) 16:e270–e278. doi: 10.1016/S1470-2045(15)70057-4
45. Shaw EG, Coffey RJ, Dinapoli RP. Neurotoxicity of radiosurgery. *Semin Radiat Oncol*. (2005) 5:235–45. doi: 10.1016/S1053-4296(05)80022-0
46. Brandes AA, Tosoni A, Spagnolli F, Frezza G, Leonardi M, Calbucci F, et al. Disease progression or pseudoprogression after concomitant radiochemotherapy treatment: pitfalls in neurooncology. *Neuro Oncol.* (2008) 10:361–7. doi: 10.1215/15228517-2008-008
47. Bian W, Hess CP, Chang SM, Nelson SJ, Lupo JM. Susceptibility-weighted MR imaging of radiation therapy-induced cerebral microbleeds in patients with glioma: a comparison between 3T and 7T. *Neuroradiology*. (2014) 56:91–6. doi: 10.1007/s00234-013-1297-8
48. Kumar AJ, Leeds NE, Fuller GN, Van Tassel P, Maor MH, Sawaya RE, et al. Malignant gliomas: MR imaging spectrum of radiation therapy- and chemotherapy-induced necrosis of the brain after treatment. *Radiology*. (2000) 217:377–84. doi: 10.1148/radiology.217.2.r00nv36377
49. Minniti G, Clarke E, Lanzetta G, Osti MF, Trasimeni G, Bozzao A, et al. Stereotactic radiosurgery for brain metastases: analysis of outcome and risk of brain radionecrosis. *Radiat Oncol*. (2001) 6:48. doi: 10.1186/1748-717X-6-48
50. Blonigen BJ, Steinmetz RD, Levin L, Lamba MA, Warnick RE, Breneman JC. Irradiated volume as a predictor of brain radionecrosis after linear accelerator stereotactic radiosurgery. *Int J Radiat Oncol Biol Phys*. (2010) 77:996–1001. doi: 10.1016/j.ijrobp.2009.06.006
51. Koike Y, Hosoda H, Ishiwata Y, Sakata K, Hidaka K. Effect of radiosurgery using Leksell gamma unit on metastatic brain tumor—autopsy case report. *Neurol Med Chir*. (1994) 34:534–7. doi: 10.2176/nmc.34.534
52. Mullins ME, Barest GD, Schaefer PW, Hochberg FH, Gonzalez RG, Lev MH. Radiation necrosis versus glioma recurrence: conventional MR imaging clues to diagnosis. *Am J Neuroradiol*. (2005) 26:1967–72. Available online at: http://www.ajnr.org/content/26/8/1967.long
53. Shah R, Vattoth S, Jacob R, Manzil FF, O'Malley JP, Borghei P, et al. Radiation necrosis in the brain: imaging features and differentiation from tumor recurrence. *Radiographics*. (2012) 32:1343–59. doi: 10.1148/rg.325125002
54. Chiang IC, Kuo YT, Lu CY, Yeung KW, Lin WC, Sheu FO, et al. Distinction between high-grade gliomas and solitary metastases using peritumoral 3-T magnetic resonance spectroscopy, diffusion, and perfusion imagings. *Neuroradiology*. (2004) 46:619–27. doi: 10.1007/s00234-004-1246-7
55. Kuesel AC, Sutherland GR, Halliday W, Smith IC. 1H MRS of high grade astrocytomas: mobile lipid accumulation in necrotic tissue. *NMR Biomed*. (1994) 7:149–55. doi: 10.1002/nbm.1940070308
56. Hatzoglou V, Yang TJ, Omuro A, Gavrilovic I, Ulaner G, Rubel J, et al. A prospective trial of dynamic contrast-enhanced MRI perfusion and fluorine-18 FDG PET-CT in differentiating brain tumor progression from radiation injury after cranial irradiation. *Neuro Oncol*. (2015) 18:873–80. doi: 10.1093/neuonc/nov301
57. Hardee MR, Zagzag D. Mechanisms of glioma-associated neovascularization. *Am J Pathol*. (2012) 181:1126–41. doi: 10.1016/j.ajpath.2012.06.030
58. Jain R, Narang J, Sundgren PM, Hearshen D, Saksena S, Rock JP, et al. Treatment induced necrosis versus recurrent/progressing brain tumor: going beyond the boundaries of conventional morphologic imaging. *J Neuro Oncol*. (2010) 100:17–29. doi: 10.1007/s11060-010-0139-3
59. Salama GR, Heier LA, Patel P, Ramakrishna R, Magge R, Tsiouris AJ. Diffusion weighted/tensor imaging, functional MRi and Perfusion weighted imaging in glioblastoma—foundations and future." *Front Neurol*. (2018) 8:660. doi: 10.3389/fneur.2017.00660
60. Barajas RF, Chang JS, Sneed PK, Segal MR, McDermott MW, Cha S. Distinguishing recurrent intra-axial metastatic tumor from radiation necrosis following gamma knife radiosurgery using dynamic susceptibility-weighted contrast-enhanced perfusion MR imaging. *Am J Neuroradiol*. (2009) 30:367–72. doi: 10.3174/ajnr.A1362
61. Falini A, Calabrese G, Origgi D, Lipari S, Triulzi F, Losa M, et al. Proton magnetic resonance spectroscopy and intracranial tumours: clinical perspectives. *J Neurol*. (1996) 243:706–14. doi: 10.1007/BF00873976
62. Donaldson SS. The power of partnerships: a message for all radiologists. *Radiology*. (2014) 271:315–9. doi: 10.1148/radiol.14140272

Conflict of Interest: The authors declare that the research was conducted in the absence of any commercial or financial relationships that could be construed as a potential conflict of interest.